

1 **Predicting ‘outbreak’-level tornado counts and casualties from**
2 **environmental variables**

3 Zoe Schroder*

4 *Department of Geography, Florida State University, Tallahassee, FL, USA, 32306*

5 James B. Elsner

6 *Florida State University, Tallahassee, FL, USA, 32306*

7 * *Corresponding author: Zoe Schroder, zms17b@my.fsu.edu*

8 * *This paper is currently under review in the Journal of Weather and Forecasting.*

ABSTRACT

9 Environmental variables are routinely used to forecast when and where an outbreak of tornadoes
10 is likely to occur but more work is needed to understand how characteristics of severe weather
11 outbreaks vary with environmental variables. Here the authors propose a method to quantify
12 ‘outbreak’-level tornado and casualty counts from environmental conditions. They do this by fitting
13 negative binomial regression models to cluster-level tornado data that estimate tornado counts and
14 associated casualties on days with at least ten tornadoes. Results show that a 1000 J kg^{-1} increase
15 in CAPE corresponds to a 5% increase in tornado counts and a 28% increase in casualties holding
16 the other variables constant. Results also show that a 10 m s^{-1} increase in deep-layer bulk shear
17 corresponds to a 13% increase in tornado counts and a 98% increase in casualties holding the other
18 variables constant. The casualty-count model quantifies the decline in the number of casualties per
19 year and indicates that tornado outbreaks have a significantly larger impact in the Southeast than
20 elsewhere after controlling for population and outbreak size.

21 **1. Introduction**

22 Predicting specific characteristics of severe weather outbreaks is an important but challenging
23 problem. Guidance from dynamical models helps forecasters outline areas of severe weather
24 threats days in advance. Guidance from statistical models help forecasters quantify probabilities
25 for given severe weather events (Hitchens and Brooks 2014; Thompson et al. 2017; Cohen et al.
26 2018; Elsner and Schroder 2019; Hill et al. 2020). For example, Cohen et al. (2018) develop a
27 regression model to specify the probability of tornado occurrence given certain environmental and
28 storm-scale conditions, and Elsner and Schroder (2019) extend this model by making use of the
29 cumulative logistic link function that predicts probabilities for each damage rating.

30 These studies put statistical guidance for predicting severe weather outbreak characteristics on a
31 firm mathematical foundation, yet there is room for additional work. For instance, the cumulative
32 logistic regression provides a distribution for the *percentage* of tornadoes within each Enhanced
33 Fujita (EF) rating category, but the regression model is silent concerning the expected overall
34 number of tornadoes. Here we propose a method to model ‘outbreak’-level tornado and casualty
35 counts from environmental conditions. The model allows us to quantify the interrelationships
36 between environmental variables and tornado counts. It also helps in extending the available
37 statistical guidance because output from a model that estimates the number of tornadoes together
38 with output from the cumulative logistic model provides a prediction for the expected number of
39 tornadoes by each EF category. Suppose for example that given current environmental conditions
40 a model predicts the distribution for the total number of tornadoes centered on fifteen while the
41 cumulative logistic regression model predicts that for each tornado there is a fifty percent chance
42 of it being EF0, a ten percent chance of it being EF1, a five percent chance of it being EF2, and

43 so on. Then a numerical convolution of these two distributions provides an expected number of
44 counts by EF rating as well as the associated uncertainties.

45 This paper has two objectives: (1) to demonstrate that environmental conditions prior to the
46 occurrence of any tornadoes can be modeled to skillfully estimate the number of tornadoes in a
47 big outbreak (tornado-count model), and (2) to show that these same environmental conditions
48 can be used to estimate the number of casualties if the number of people in harm's way is known
49 (casualty-count model). We accomplish these objects by fitting negative binomial regressions to
50 cluster-level tornado data. The data are environmental variables and tornado characteristics (e.g.,
51 number of tornadoes, area of cluster, etc) on 'big' convective days (12 UTC to 12 UTC), when the
52 number of tornadoes is at least ten (see Elsner and Schroder (2019)).

53 The models show that a 1000 J kg^{-1} increase in CAPE results in a 4.7% increase in the expected
54 number of tornadoes and a 28% increase in the expected number of casualties holding the other
55 variables constant. Further models show that a 10 m s^{-1} increase in deep-layer bulk shear results
56 in a 13% increase in the expected number of tornadoes and a 98% increase in the expected
57 number of casualties holding the other variables constant. The casualty-count model also shows a
58 significant decline in the number of casualties at a rate of 3.6% per year and that expected casualties
59 depend on where the outbreak occurs with more casualties on average over the Southeast all else
60 being equal. The paper is outlined as follows. The data and methods are discussed in section 2
61 including the mathematics of a negative binomial regression. Statistics describing the response
62 and environmental variables are given in section 3. The modeling results are presented in section
63 4, and a summary with conclusions are given in section 5.

64 2. Data and methods

65 We fit regression models to a set of reanalysis data aggregated to the level of tornado clusters.
66 Here we describe the available data and the procedures we use to aggregate representative values to
67 the cluster level. For our purposes, a cluster is a space-time group of at least ten tornadoes occurring
68 between 12 UTC and 12 UTC. Ten is chosen as a compromise between too few clusters leading
69 to greater uncertainty and too many clusters leading to excessive time required to fit the models
70 (Elsner and Schroder 2019). The number of tornadoes in each cluster is the response variable in
71 the tornado-count regression model, and the number of casualties is the response variable in the
72 casualty-count regression model. Explanatory variables for the models are taken from reanalysis
73 data representing the environment before the occurrence of the first tornado in the cluster.

74 *a. Tornado clusters*

75 First, we extract the date, time, genesis location, and magnitude of all tornado reports between
76 1994 and 2018 from the Storm Prediction Center [SPC] (<https://www.spc.noaa.gov/gis/svrgis/>). We choose 1994 as the start year because it is the first year of the extensive use of the
77 WSR-88D Radar. Each row in the data set contains information at the individual tornado level.
78 In total, there are 30 497 tornado reports during this period. The geographic coordinates for each
79 genesis location are converted to Lambert conic conformal coordinates, where the projection is
80 centered on 107° W longitude.

82 Next, we assign to each tornado a cluster identification number based on the space and time
83 differences between genesis locations. Two tornadoes are assigned the same cluster identification
84 number if they occur close together in space and time (e.g., 1 km and 1 h). When the difference
85 between individual tornadoes and existing clusters surpasses 50 000 s (~ 14 h), the clustering
86 ends. The space-time differences have units of seconds because we divide the spatial distance

87 by 15 m s^{-1} to account for the average speed of tornado-producing storms. This clustering of
88 tornadoes is identical to that used in Elsner and Schroder (2019) who fit a cumulative logistic
89 model to the damage scale at the individual tornado level. Additional details on the procedure as
90 well as a comparison of the identified clusters to well-known tornado outbreaks are available in
91 Schroder and Elsner (2019).

92 We keep only clusters that have at least ten tornadoes occurring within the same convective day,
93 which results in 768 clusters containing a total of 17 069 tornadoes. A convective day is defined as a
94 24-hour period beginning at 1200 UTC (Doswell III et al. 2006). The average number of tornadoes
95 (for clusters with at least ten tornadoes) is 22 tornadoes and the maximum is 173 tornadoes (April
96 27, 2011). There are 80 clusters with exactly ten tornadoes. Each cluster varies by area and by
97 where it occurs (Fig. 1). The cluster area is defined by the minimum convex hull (black polygon)
98 that includes all the tornado genesis locations. The July 19, 1994 cluster with nine tornadoes over
99 northern Iowa and one over northeast Wisconsin had an area of $33\,359 \text{ km}^2$ and lasted about four
100 hours. The April 27, 2011 cluster had 173 tornadoes spread over more than a dozen states and
101 had an area of $1\,064\,337 \text{ km}^2$ with tornadoes occurring throughout the 24-h period (12-UTC to
102 12-UTC).

103 For each cluster we sum the number of injuries and deaths across all tornadoes to get the cluster-
104 level number of casualties. Further we estimate the total population within the cluster area and the
105 geographic center of the cluster. Population is used as an explanatory variable in place of cluster
106 area when the number of casualties is the dependent variable.

107 *b. Environmental variables*

108 Environmental conditions for producing tornadoes are well known and include high values of
109 convective available potential energy, convective inhibition, and bulk shear (Brooks et al. 1994;

110 Rasmussen and Blanchard 1998; Tippett et al. 2012, 2014; Elsner and Schroder 2019). We
111 obtain variables associated with these environmental conditions from the National Centers for
112 Atmospheric Research’s North American Regional Reanalysis (NARR) which is supported by
113 the National Centers for Environmental Prediction. Each variable has numeric values given on
114 a 32-km raster grid with the values available in three-hour increments starting at 00 UTC. We
115 note that in the severe weather literature these environmental variables are called ‘parameters’.
116 However here, since we employ statistical models, we prefer to call them variables to be consistent
117 with the statistical literature where the word ‘parameter’ denotes unknown model coefficients and
118 distributional moments.

119 We select environmental variables at the nearest three-hour time *prior* to the occurrence of the
120 first tornado in the cluster. For example, if the first tornado in a cluster occurs at 16:30 UTC we
121 use the environmental variables given at 15 UTC. This selection criteria results in a sample of the
122 environment that is less contaminated by the deep convection itself but at a cost that underestimates
123 the severity in cases where rapid increases in conditions favoring tornadoes occur. We note that
124 roughly 60% of all clusters have the initial tornado occurring between 18 and 00 UTC (Table 1).
125 We also note that there are more tornadoes on average in clusters where the first tornado occurs
126 between 15 and 18 UTC.

127 The environmental variables we consider in this study include convective available potential
128 energy (CAPE) and convective inhibition(CIN) as computed using the near-surface layer (0 to 180
129 mb above the ground level) as well as deep (1000 to 500 mb) and shallow (1000 to 850 mb) layer
130 bulk shears (DLBS, SLBS) computed as the square root of the sum of the squared differences
131 between the u and v wind components at the respective levels. We take the highest (lowest for CIN)
132 value across the grid of values within the area defined by the cluster’s convex hull. This is done
133 to capture the extremes of the environmental condition. The maximum values within a cluster

134 provide a better representation of the environments since they are not substantially influenced by
135 meso-scale phenomena unrelated to tornado genesis.

136 *c. Negative binomial regression*

137 With the cluster as our unit of analysis we fit a series of regression models to the data having the
138 form

$$T \sim \text{NegBin}(\hat{\mu}, n)$$
$$\ln(\hat{\mu}) = \beta_0 + \beta_A A + \beta_\phi \phi + \beta_\lambda \lambda + \beta_Y Y + \beta_{CAPE} CAPE + \beta_{CIN} CIN + \beta_{DLBS} DLBS + \beta_{SLBS} SLBS, \quad (1)$$

139 where the number of tornadoes (T) (or number of casualties C) is the dependent variable that
140 is assumed to be adequately described by a negative binomial distribution (NegBin) with a rate
141 parameter μ and a size parameter n . The natural logarithm of the rate parameter is linearly related
142 to cluster area (A), cluster center location [latitude (ϕ) and longitude (λ)], year (Y) and the four
143 environmental variables (CAPE, CIN, DLBS, and SLBS). The model is fit using the method of
144 maximum likelihoods carried out in the call to the `glm.nb` function from {MASS} package in R.
145 We do the same for the initial casualty-count model, but we replace cluster area with population
146 (P). We simplify the initial models by single-term deletions as described in §4.

147 **3. Descriptive statistics**

148 The number of clusters decreases exponentially with an increasing number of tornadoes (Fig. 2).
149 There are 80 clusters with ten tornadoes but only ten clusters with 30 tornadoes. The right tail of
150 the count distribution is long with the April 27, 2011 cluster having 173 tornadoes [47 (6%) of
151 the clusters have more than 50 tornadoes and are not shown]. However more clusters have 20 or
152 21 tornadoes than expected from this exponential decay. This deviation is unlikely the result of

153 physical processes and it appears too large to be sampling variability. The distribution of casualties
154 is also skewed toward many clusters having only a few casualties and a few have many. Thirty-six
155 percent of all clusters (275) are without a casualty and 56% of the clusters have fewer than four
156 casualties.

157 There is a distinct seasonality to the chance of at least one tornado cluster (Fig. 3). The empirical
158 seven-day probability of at least one cluster is between 20 and 30% for much of the year except
159 between the middle of March and early July. The probabilities approach 80% between mid and
160 late May. The number of tornadoes per cluster is less variable ranging between about 10 and 35
161 tornadoes per week with no strong seasonality although clusters during July and August tend to
162 have somewhat fewer tornadoes. The casualty rate, defined as the number of casualties per 100,000
163 people within the cluster area, shows a distinct seasonality with rates being highest between late
164 January through late May.

165 Across the 768 clusters the mean value of regionally highest CAPE is $2\,225\text{ J kg}^{-1}$ and the mean
166 value of regionally lowest CIN is -114 J kg^{-1} (Table 2). The maximum deep-layer bulk shear
167 values range from 5.6 to 47.9 m s^{-1} . Cluster areas range from 361 to $1\,064\,337\text{ km}^2$ with an
168 average of $167\,990\text{ km}^2$.

169 **4. Results**

170 *a. A model for the number of tornadoes*

171 First we fit a negative binomial regression to the cluster-level tornado counts using the explanatory
172 variables given in Table 2. This is our tornado-count model. We divide the cluster area by 10
173 million so it has units of 100 km^2 . We divide CAPE by 1000 so it has units of 1000 J kg^{-1} and

174 we divide CIN by 100 so it has units of 100 J kg^{-1} . This simplifies interpretation of the model
175 coefficients.

176 All terms have signs on the coefficient that make physical sense (Table 3). The number of
177 tornadoes in a cluster increases with cluster area, CAPE, and bulk shear (deep and shallow layers)
178 and decreases for increasing values of CIN as expected. The significance of the variable in
179 statistically explaining tornado counts is assessed by the corresponding z -value given as the ratio
180 of the coefficient estimate to its standard error (S.E.). We reject the null hypothesis that a particular
181 variable has no explanatory power if its corresponding p -value is less than .01. Here we fail to
182 reject the null hypothesis for the variables latitude, longitude, and year, which indicates that these
183 non-physical variables have a relatively small impact on tornado counts relative to the physical
184 variables given the data and the model. In particular, there is no significant upward or downward
185 trend over time in the number of tornadoes in these clusters. The only physical variable that is
186 not statistically significant is CIN. We remove all statistically insignificant variables before fitting
187 a final model.

188 All variables in the final model are significant although the coefficients have changed a bit
189 relative to the initial model. The in-sample correlation between the observed counts and predicted
190 rates is .59 [(0.54, 0.64), 95% uncertainty interval (UI)] (Fig. 4). The model statistically explains
191 almost 60% of the variation in cluster-level tornado counts but tends to over predict the number of
192 tornadoes for smaller clusters and slightly under predict the number of tornadoes for larger clusters.
193 The mean absolute error between the observed counts and expected rates is 8.6 tornadoes or 5.2%
194 of the range in observed counts and 9.3% of the range in predicted rates. The out-of-sample
195 errors are quite similar due to the large sample size (768 clusters). A hold-one-out cross validation
196 exercise (Elsner and Schmertmann 1994) results in an out-of-sample correlation of .58 and a mean
197 absolute error of 8.6 tornadoes.

198 The β_0 value (Table 3) is the regression estimate when all variables in the model are evaluated at
 199 zero. The effect size for a given explanatory variable is given by the magnitude of its coefficient.
 200 The coefficient is expressed as the difference in the logarithm of the expected tornado counts for
 201 a unit increase in the explanatory variable holding the other variables constant. For example, the
 202 scaled units of CAPE are 1000 J kg^{-1} . An increase in CAPE of 1000 J kg^{-1} results in a $[(\exp(.0459)$
 203 $- 1) \times 100\% = 4.7\%$ increase in the expected number of tornadoes. Continuing, units of deep-layer
 204 bulk shear are 10 m s^{-1} so an increase in shear of 10 m s^{-1} results in a 13% increase in the expected
 205 number of tornadoes. A similar increase in shallow-layer bulk shear results in a 11.1% increase in
 206 the number of tornadoes.

207 Changes to the expected number of tornadoes given changes in the environmental variables
 208 have a large impact on the probability distribution of counts conditional on the cluster area. The
 209 negative binomial distribution for the number of tornadoes T with an expected number of tornadoes
 210 \bar{T} (obtained from the regression model) has a probability density

$$\Pr(T = k) = \frac{\Gamma(r+k)}{k! \Gamma(r)} \left(\frac{r}{r+\bar{T}} \right)^r \left(\frac{\bar{T}}{r+\bar{T}} \right)^k \quad \text{for } k = 10, 11, 12, \dots, \quad (2)$$

211 where $r = 1/n$ and $\Gamma(z) = \int_0^\infty x^{z-1} e^{-x} dx$ is the gamma function.

212 For example, on April 12, 2020 the 12 UTC guidance from SPC outlined a polygon that defined
 213 an area with a 10% chance of at least one tornado occurring within 46 km of any location (10%
 214 tornado risk). The area of the polygon was approximately $400\,000 \text{ km}^2$ (much larger than the
 215 average cluster area) centered on Mississippi. With an area of that size, the model estimates the
 216 probability of at least 30 tornadoes for a range of deep-layer shear values and conditional on the
 217 amount of CAPE while holding shallow-layer shear at an average value (Fig. 5). Given an average
 218 amount of shallow-layer shear, a deep-layer shear of 10 m s^{-1} and low CAPE (5th percentile value),
 219 the model predicts a 17% [9, 26%, UI] chance of at least 30 tornadoes (given a cluster with at least

220 ten tornadoes). In contrast, given a deep-layer shear of 40 m s^{-1} and high CAPE (95th percentile
221 value), the model predicts a 65% [(56, 71%), UI] chance of at least 30 tornadoes. There were at
222 least 100 tornado numbers on that day.

223 The procedure quantifies the relationship between CAPE and shear in terms of a probability
224 distribution on the number of tornadoes. The regression model predicts the expected count
225 given values for the explanatory variables. The negative binomial distribution uses the model
226 predicted count and the size parameter to generate a distribution of probabilities. For example,
227 the procedure outputs predicted probabilities across a range of CAPE and deep-layer shear values
228 (holding shallow-layer shear at its mean value) that provides a high resolution picture of the modeled
229 relationship (Fig. 6). The predicted probabilities of at least 30 tornadoes given an outbreak covering
230 an area of $400\,000 \text{ km}^2$ increase from low values of both CAPE and shear to high values of both
231 CAPE and shear.

232 *b. A model for the number of casualties*

233 Next we fit a negative binomial regression to the cluster-level casualty counts (direct injuries and
234 deaths) using the same explanatory variables (Table 2) with the exceptions that population (scaled
235 by 100,000 residents) replaces cluster area and C (casualty count) replaces T (tornado count) as
236 the dependent variable. This is our casualty-count model. We find that CIN is the only variable
237 not significant in the initial model (Table 4). We remove it before fitting a final model.

238 The in-sample correlation between the observed casualty counts and predicted rates is .43 [(0.37,
239 .48), 95% UI] (Fig. 7). The mean absolute error between the observed counts and expected rates
240 is 39 casualties or 1.3% of the range in observed counts and 3.4% of the range in predicted rates.
241 The out-of-sample correlation is .36 and the mean absolute error is 40 casualties. The skill is

242 lower than the skill of the tornado-count model as there is additional uncertainty associated with
243 the number of casualties given a tornado.

244 As expected, based on the model for the number of tornadoes, the number of casualties resulting
245 from a cluster of tornadoes increases with CAPE and with the two bulk shear variables (Table 4).
246 Holding all other variables constant, an increase in CAPE of 1000 J kg^{-1} results in a 28% increase
247 in the expected number of casualties. An increase in deep-layer bulk shear of 10 m s^{-1} results in
248 a 98% increase in the expected number of casualties and a similar increase in shallow-layer bulk
249 shear results in a 76% increase in the expected number of casualties. There is also a significant
250 downward trend (negative value for the β_Y coefficient) in the number of casualties at a rate of 3.6%
251 per year. This is very likely the result of improvements made by the National Weather Service
252 in warning coordination and dissemination leading to better awareness especially for these large
253 outbreak events.

254 Also as expected the number of people in harm's way is a significant predictor for the cluster-level
255 casualty count. The relationship between population and number of casualties is quantified at the
256 tornado-level in Elsner et al. (2018) and Fricker et al. (2017) so we expect it to hold at the cluster
257 level. But here for the first time, we are able to compare the influence of shear and CAPE on the
258 probability of casualties as modulated by population (Fig. 8). Model results are shown for three
259 levels of population. The probability of a large number of casualties increases with increasing
260 shear and increasing CAPE while keeping the other variables at their mean values and year at 2018.

261
262 Importantly, we also find that the location of the cluster has a significant influence on the number
263 of casualties. For every one degree north latitude the casualty rate decreases by 5.5% and for every
264 one degree east longitude the casualty rate increases by 2.9%. Thus cluster-level casualties are
265 highest over the Southeast. This effect is independent of the number tornadoes since location was

266 not a significant factor in the tornado-count model. The result is also independent of the number
267 of people in harm's way since population is included as an exploratory variable in the model.

268 To visualize the difference the combine effects of latitude and longitude on the difference in the
269 probability of many casualties, we plot modeled casualty probabilities (at least 25) as function of
270 CAPE and deep-layer shear for two *hypothetical* outbreaks that are the same in every way except
271 one outbreak is center on Sioux City, Iowa and the other is centered on Birmingham, Alabama
272 (Fig. 9). The modeled probabilities are lowest (around 5%) for low CAPE and shear values and
273 highest (above 30%) for high CAPE and shear values. The difference in modeled probabilities
274 across these two locations peaks at about +12 percentage points for high CAPE and high shear
275 regimes when the outbreak is centered over Birmingham.

276 5. Summary and conclusions

277 Forecasting characteristics of severe weather outbreaks is challenging. Forecasters use a combi-
278 nation of numerical weather prediction and empirical guidance to outline areas of severe convective
279 weather. Machine learning algorithms are now routinely employed for these tasks particularly when
280 the focus is on prediction rather than on explanation. Here we demonstrate how to employ a statis-
281 tical regression model to take advantage of the large sample of independent tornado-day events as
282 a way to parsimoniously predict and importantly to statistically explain the number of tornadoes
283 and the number of casualties in an outbreak.

284 We fit negative binomial regressions to observational data aggregated to the level of tornado
285 clusters where a cluster is a space-time group of at least ten tornadoes occurring between 12
286 UTC and 12 UTC over the period 1994–2018. The number of tornadoes in each cluster is the
287 response variable in the tornado-count model and the number of casualties (deaths plus injuries)
288 is the response variable in the casualty-count model. Environmental explanatory variables for the

289 models are extracted from reanalysis data representing conditions before the occurrence of the
290 first tornado in the cluster. Additional explanatory variables including cluster area, population,
291 location, and year.

292 The predicted tornado rates explain 59% of the observed tornado counts in-sample, and the
293 predicted casualty rates explain 43% of the observed casualty counts in-sample. Because of
294 the large sample size the out-of-sample skill is lower, but still useful. The models show that a
295 1000 J kg^{-1} increase in CAPE results in a 4.7% increase in the expected number of tornadoes and
296 a 28% increase in the expected number of casualties holding the other variables constant. The
297 models further show that a 10 m s^{-1} increase in deep-layer bulk shear results in a 13% increase
298 in the expected number of tornadoes and a 98% increase in the expected number of casualties
299 holding the other variables constant. The casualty-count model also shows a significant decline
300 in the number of casualties at a rate of 3.6% per year. And casualty rates depend on where the
301 outbreak occurs with more deaths and injuries, on average, over the Southeast controlling for the
302 other variables.

303 Some of the unexplained variability in cluster-level tornado counts (and thus casualty counts)
304 arises from the uncertainty associated with the preferred storm mode and the evolution of meso-
305 scale convective systems neither of which are captured by a single maximum value in the variable
306 space of CAPE and shear. Also outbreaks associated with tropical cyclones likely add a bit of noise
307 to both models since the number of tornadoes is sensitive to the extent and location of convective
308 bursts within overall evolution of the land-falling storm. In addition, the casualty-count model
309 would be improved by including a skillful prediction of the number of tornadoes. Indeed in a
310 perfect-prognostic setting where we know the number of tornadoes in the outbreak, the out-of-
311 sample correlation between the observed number of casualties and the modeled estimated rate of
312 casualties increases to .79.

313 A tornado-count model like the one demonstrated here might assist forecast guidance given a
314 convective outlook that highlights an area of elevated risk for tornadoes and a dynamical forecast of
315 CAPE and shear across the elevated-risk area. The statistical model would need to be calibrated for
316 forecast areas and environmental variables but the exact same model equation used here will provide
317 a probability distribution on the future number of tornadoes that should retain some level of skill.
318 Further, a numerical convolution of this probability distribution with a probability distribution for
319 each EF-rating category (Elsner and Schroder 2019) will give a forecast of the expected number
320 of counts by category as well as the associated uncertainties. Similarly the casualty-count model
321 might prove useful for communicating the risk given the population within the elevated risk area.

322 The casualty-count model can also be employed in a research setting to help better understand the
323 socioeconomic, demographic, and communication factors that make some communities particularly
324 vulnerable to deaths and injuries (Dixon and Moore 2012; Senkbeil et al. 2013; Klockow et al.
325 2014; Fricker and Elsner 2019). Work along this line has been done at the individual tornado
326 level by identifying unusually devastating events (Fricker and Elsner 2019) but scaling this type of
327 analysis to the cluster-level to identify unusually devastating outbreaks might provide additional
328 insights.

329 Finally, the model specifications might be improved by adjusting the threshold definition of a
330 cluster. Increasing the threshold on the tornado-count model from 10 to 14 decreases the sample
331 size to 505 clusters and reduces the effect sizes on CAPE and shear by around 25%. Decreasing
332 the threshold from 10 to 6 increases the sample size and thus reduces the standard error assuming
333 the effect size stays the same. The casualty-count model might also be improved by relaxing the
334 assumption that the number of people injured or killed are independent. Casualties counts are
335 typically not independent at the household level where multiple people live under the same roof.

³³⁶ In this case a zero-inflated count model might be provide a better fit to the data compared with a
³³⁷ negative binomial distribution count model.

References

- Brooks, H. E., C. A. Doswell III, and J. Cooper, 1994: On the environments of tornadic and nontornadic mesocyclones. *Weather and Forecasting*, **9**, 606–618, doi:10.1175/1520-0434.
- Cohen, A. E., J. B. Cohen, R. L. Thompson, and B. T. Smith, 2018: Simulating tornado probability and tornado wind speed based on statistical models. *Weather and Forecasting*, **33** (4), 1099–1108, doi:10.1175/waf-d-17-0170.1, URL <https://doi.org/10.1175/waf-d-17-0170.1>.
- Dixon, R. W., and T. W. Moore, 2012: Tornado vulnerability in Texas. *Weather, Climate, and Society*, **4**, 59–68.
- Doswell III, C. A., R. Edwards, R. L. Thompson, J. A. Hart, and K. C. Crosbie, 2006: A simple and flexible method for ranking severe weather events. *Weather and Forecasting*, **21** (6), 939–951, doi:10.1175/waf959.1, URL <https://doi.org/10.1175/waf959.1>.
- Elsner, J. B., T. Fricker, and W. D. Berry, 2018: A model for u.s. tornado casualties involving interaction between damage path estimates of population density and energy dissipation. *Journal of Applied Meteorology and Climatology*, **57**, 2035–2046.
- Elsner, J. B., and C. P. Schertmann, 1994: Assessing forecast skill through cross validation. *Weather and Forecasting*, **9** (4), 619–624.
- Elsner, J. B., and Z. Schroder, 2019: Tornado damage ratings estimated with cumulative logistic regression. *Journal of Applied Meteorology and Climatology*, **58** (12), 2733–2741, doi:10.1175/jamc-d-19-0178.1, URL <https://doi.org/10.1175/jamc-d-19-0178.1>.
- Fricker, T., and J. B. Elsner, 2019: Unusually devastating tornadoes in the united states: 1995–2016. *Annals of the American Association of Geographers*, **110** (3), 724–738, doi:10.1080/24694452.2019.1638753, URL <https://doi.org/10.1080/24694452.2019.1638753>.

360 Fricker, T., J. B. Elsner, and T. H. Jagger, 2017: Population and energy elasticity of tornado
361 casualties. *Geophysical Research Letters*, **44**, 3941–3949, doi:10.1002/2017GL073093.

362 Hill, A. J., G. R. Herman, and R. S. Schumacher, 2020: Forecasting severe weather with random
363 forests. *Monthly Weather Review*, doi:10.1175/mwr-d-19-0344.1, URL [https://doi.org/10.1175/
364 mwr-d-19-0344.1](https://doi.org/10.1175/mwr-d-19-0344.1).

365 Hitchens, N. M., and H. E. Brooks, 2014: Evaluation of the Storm Prediction Center’s convective
366 outlooks from day 3 through day 1. *Weather and Forecasting*, **29** (5), 1134–1142, doi:10.1175/
367 waf-d-13-00132.1, URL <https://doi.org/10.1175/waf-d-13-00132.1>.

368 Klockow, K. E., R. A. Pepler, and R. A. McPherson, 2014: Tornado folk science in Alabama
369 and Mississippi in the 27 April 2011 tornado outbreak. *GeoJournal*, **79** (6), 791–804, doi:
370 10.1007/s10708-013-9518-6, URL <https://doi.org/10.1007/s10708-013-9518-6>.

371 Rasmussen, E. N., and D. O. Blanchard, 1998: A baseline climatology of sounding-
372 derived supercell and tornado forecast parameters. *Weather and Forecasting*, **13** (4), 1148–
373 1164, doi:10.1175/1520-0434(1998)013<1148:ABCOSD>2.0.CO;2, URL [https://doi.org/10.
374 1175/1520-0434\(1998\)013<1148:ABCOSD>2.0.CO;2](https://doi.org/10.1175/1520-0434(1998)013<1148:ABCOSD>2.0.CO;2).

375 Schroder, Z., and J. B. Elsner, 2019: Quantifying relationships between environmental factors
376 and power dissipation on the most prolific days in the largest tornado “outbreaks”. *International
377 Journal of Climatology*, doi:10.1002/joc.6388, URL <https://doi.org/10.1002/joc.6388>.

378 Senkbeil, J. C., D. A. Scott, P. Guinazu-Walker, and M. S. Rockman, 2013: Ethnic and racial
379 differences in tornado hazard perception, preparedness, and shelter lead time in Tuscaloosa. *The
380 Professional Geographer*, **66** (4), 610–620, doi:10.1080/00330124.2013.826562, URL [https:
381 //doi.org/10.1080/00330124.2013.826562](https://doi.org/10.1080/00330124.2013.826562).

382 Thompson, R. L., and Coauthors, 2017: Tornado damage rating probabilities derived from WSR-
383 88D data. *Weather and Forecasting*, **32** (4), 1509–1528, doi:10.1175/waf-d-17-0004.1, URL
384 <https://doi.org/10.1175/waf-d-17-0004.1>.

385 Tippett, M. K., A. H. Sobel, and S. J. Camargo, 2012: Association of U.S. tornado occurrence
386 with monthly environmental parameters. *Geophysical Research Letters*, **39**, L02 801.

387 Tippett, M. K., A. H. Sobel, S. J. Camargo, and J. T. Allen, 2014: An empirical relation between
388 U.S. tornado activity and monthly environmental parameters. *Journal of Climate*, **27**, 2983–
389 2999.

390 **LIST OF TABLES**

391 **Table 1.** Cluster statistics by time of day. Each cluster is categorized by the closest
392 three-hour time (defined by the NARR data) prior to the first tornado. 22

393 **Table 2.** Variables used in the regression models. Values include the range and average
394 across the 768 tornado clusters. 23

395 **Table 3.** Coefficients in the tornado-count models. The size parameter (n) is $6.27 \pm .393$
396 (S.E.) for the initial model $6.25 \pm .392$ (S.E.) for the final model. 24

397 **Table 4.** Coefficients in the casualty-county models. The size parameter (n) is $.261 \pm .014$
398 (S.E.) for the initial and final models. 25

399 TABLE 1. Cluster statistics by time of day. Each cluster is categorized by the closest three-hour time (defined
400 by the NARR data) prior to the first tornado.

Time of Day (UTC)	Number of Clusters	Number of Tornadoes	Tornadoes Per Cluster
00	33	523	15.8
03	5	67	13.4
06	2	23	11.5
12	145	3598	12.1
15	124	3222	26.0
18	249	5220	21.0
21	210	4416	21.0

401 TABLE 2. Variables used in the regression models. Values include the range and average across the 768 tornado
 402 clusters.

Variable	Abbreviation	Range	Average
Explanatory Variables			
Convective Available Potential Energy [J kg ⁻¹]	CAPE	[0, 6530]	2225
Convective Inhibition [J kg ⁻¹]	CIN	[-668, 0]	-114
Deep-Layer Bulk Shear [m s ⁻¹]	DLBS	[5.6, 48]	27.5
Shallow-Layer Bulk Shear [m s ⁻¹]	SLBS	[1.1, 33.8]	15.0
Latitude [° N]	ϕ	[27.12, 48.97]	37.20
Longitude [° E]	λ	[-109.9 -72.88]	-92.16
Cluster Area [km ²]	A	[361, 1 064 337]	167 990
Population [No. of People]	P	[0, 38 226 946]	3 387 259
Year	Y	[1994, 2018]	2006
Response Variables			
Number of Tornadoes	T	[0, 173]	22.2
Number of Casualties (injuries plus deaths)	C	[0, 3 069]	29.9

403 TABLE 3. Coefficients in the tornado-count models. The size parameter (n) is $6.27 \pm .393$ (S.E.) for the initial
 404 model $6.25 \pm .392$ (S.E.) for the final model.

Coefficient	Estimate	S.E.	z value	$\Pr(> z)$
Initial Model				
β_0	4.5489	4.7662	0.9540	0.3399
β_A	0.0146	0.0011	12.80	< 0.0001
β_ϕ	-0.0051	0.0043	-1.17	0.2427
β_λ	-0.0028	0.0031	-0.917	0.3594
β_Y	-0.0012	0.0024	-0.515	0.6068
β_{CAPE}	0.0452	0.0153	2.96	0.0031
β_{CIN}	-0.0110	0.0189	-0.581	0.5612
β_{DLBS}	0.1256	0.0292	4.30	< 0.0001
β_{SLBS}	0.1059	0.0355	2.98	0.0029
Final Model				
β_0	2.1779	0.0817	26.65	< 0.0001
β_A	0.0149	0.0011	13.85	< 0.0001
β_{CAPE}	0.0459	0.0146	3.13	0.0017
β_{DLBS}	0.1254	0.0288	4.35	< 0.0001
β_{SLBS}	0.1054	0.0314	3.35	0.0008

405 TABLE 4. Coefficients in the casualty-county models. The size parameter (n) is $.261 \pm .014$ (S.E.) for the
 406 initial and final models.

Coefficient	Estimate	S.E.	z value	$\Pr(> z)$
Initial Model				
β_0	76.6908	20.7430	3.70	0.0002
β_P	0.0122	0.0019	6.51	< 0.0001
β_ϕ	-0.0561	0.0187	-3.00	0.0027
β_λ	0.0284	0.0136	2.09	0.0363
β_Y	-0.0364	0.0103	-3.52	0.0004
β_{CAPE}	0.2436	0.0643	3.79	0.0002
β_{CIN}	0.0052	0.0802	0.07	0.9479
β_{DLBS}	0.6853	0.1262	5.43	< 0.0001
β_{SLBS}	0.5650	0.1534	3.68	0.0002
Final Model				
β_0	76.7677	20.6902	3.71	0.0002
β_P	0.0122	0.0018	6.67	0.0000
β_ϕ	-0.0563	0.0186	-3.02	0.0025
β_λ	0.0287	0.0130	2.20	0.0277
β_Y	-0.0364	0.0103	-3.53	0.0004
β_{CAPE}	0.2440	0.0643	3.79	0.0001
β_{DLBS}	0.6833	0.1253	5.45	0.0000
β_{SLBS}	0.5631	0.1504	3.74	0.0002

407 **LIST OF FIGURES**

408 **Fig. 1.** Example tornado clusters. Each point is the tornado genesis location shaded by EF rating.
 409 The black line is the spatial extent of the tornadoes occurring on that convective day and is
 410 defined by the minimum convex hull encompassing the set of genesis locations. 27

411 **Fig. 2.** Histograms of the number of clusters by number of tornadoes (A) and number of clusters by
 412 number of casualties (B). The histograms are right-truncated at 50 to show detail on the left
 413 side of the distributions. Only clusters with at least ten tornadoes are considered in this study. 28

414 **Fig. 3.** Probability of a cluster, average number of tornadoes per cluster, and average number of
 415 casualties per million people per cluster by week of the year. 29

416 **Fig. 4.** Observed cluster-level tornado counts versus predicted rates from a negative binomial re-
 417 gression. 30

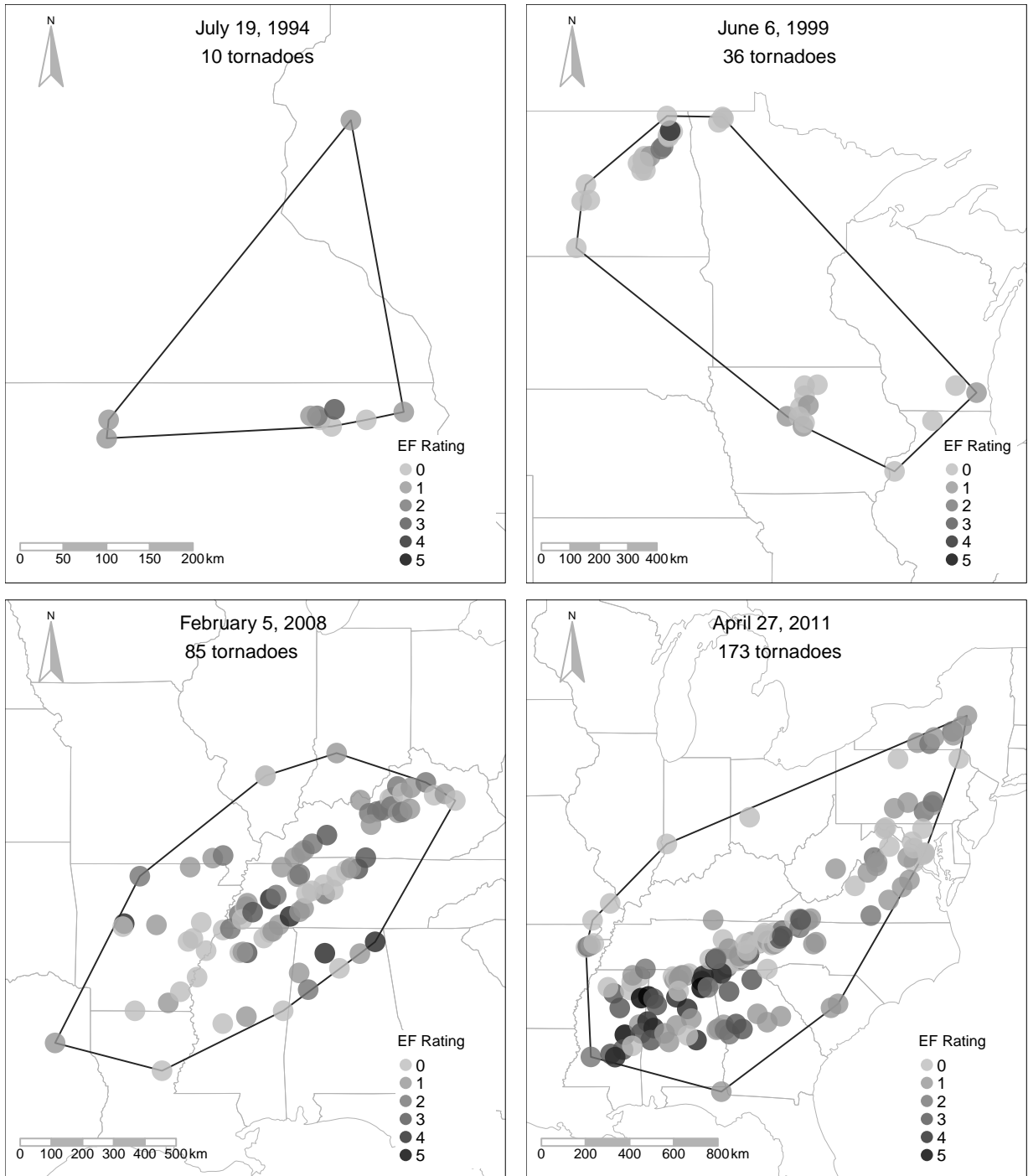
418 **Fig. 5.** Estimated probability of at least 30 tornadoes given an outbreak of at least ten tornadoes
 419 and the regression model. The predicted count from the model is a parameter in a negative
 420 binomial distribution with cluster area set at 400 000 km² and shallow-level bulk shear is set
 421 to its mean value. 31

422 **Fig. 6.** Estimated probability of at least 30 tornadoes given an outbreak of at least ten tornadoes and
 423 the regression model across a range of CAPE and deep-layer bulk shear values holding the
 424 shallow-layer bulk shear at a mean value. 32

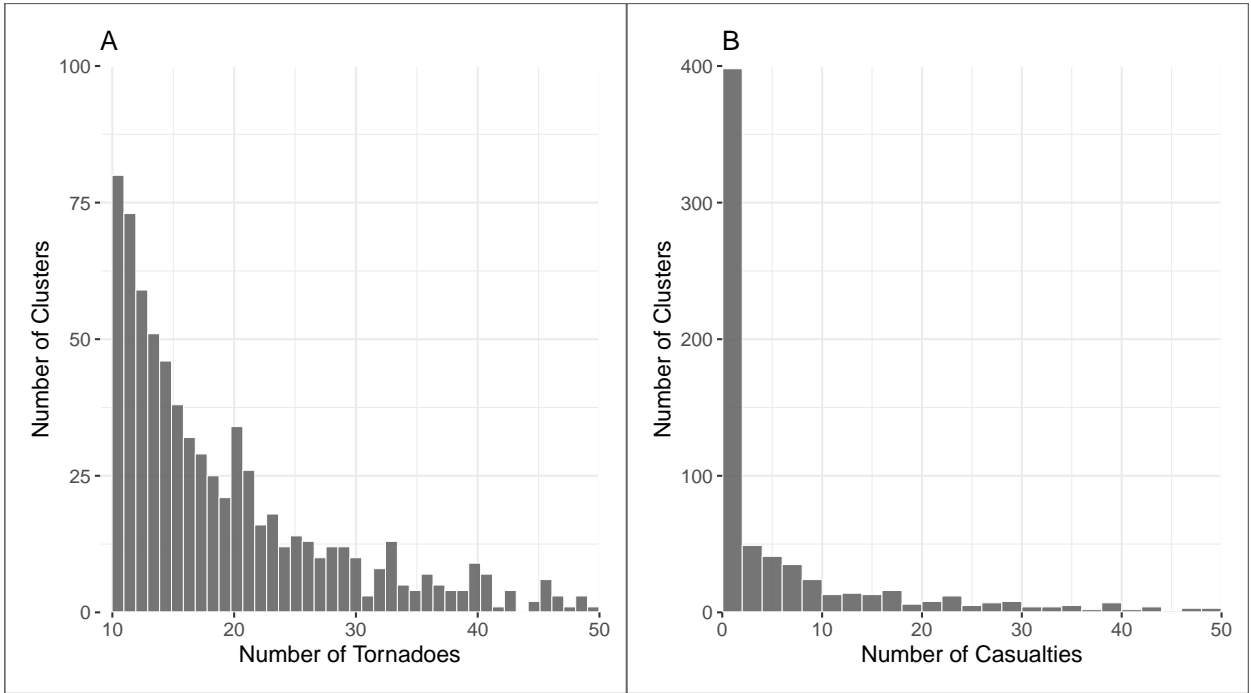
425 **Fig. 7.** Observed cluster-level casualty counts versus predicted rates from a negative binomial re-
 426 gression. Clusters without casualties are plotted at the far left. 33

427 **Fig. 8.** Probability of at least 50 tornado casualties as a function of deep-layer bulk shear and CAPE
 428 and modulated by the number of people in harms way. The other variables are set at their
 429 mean values and year is set at 2018. 34

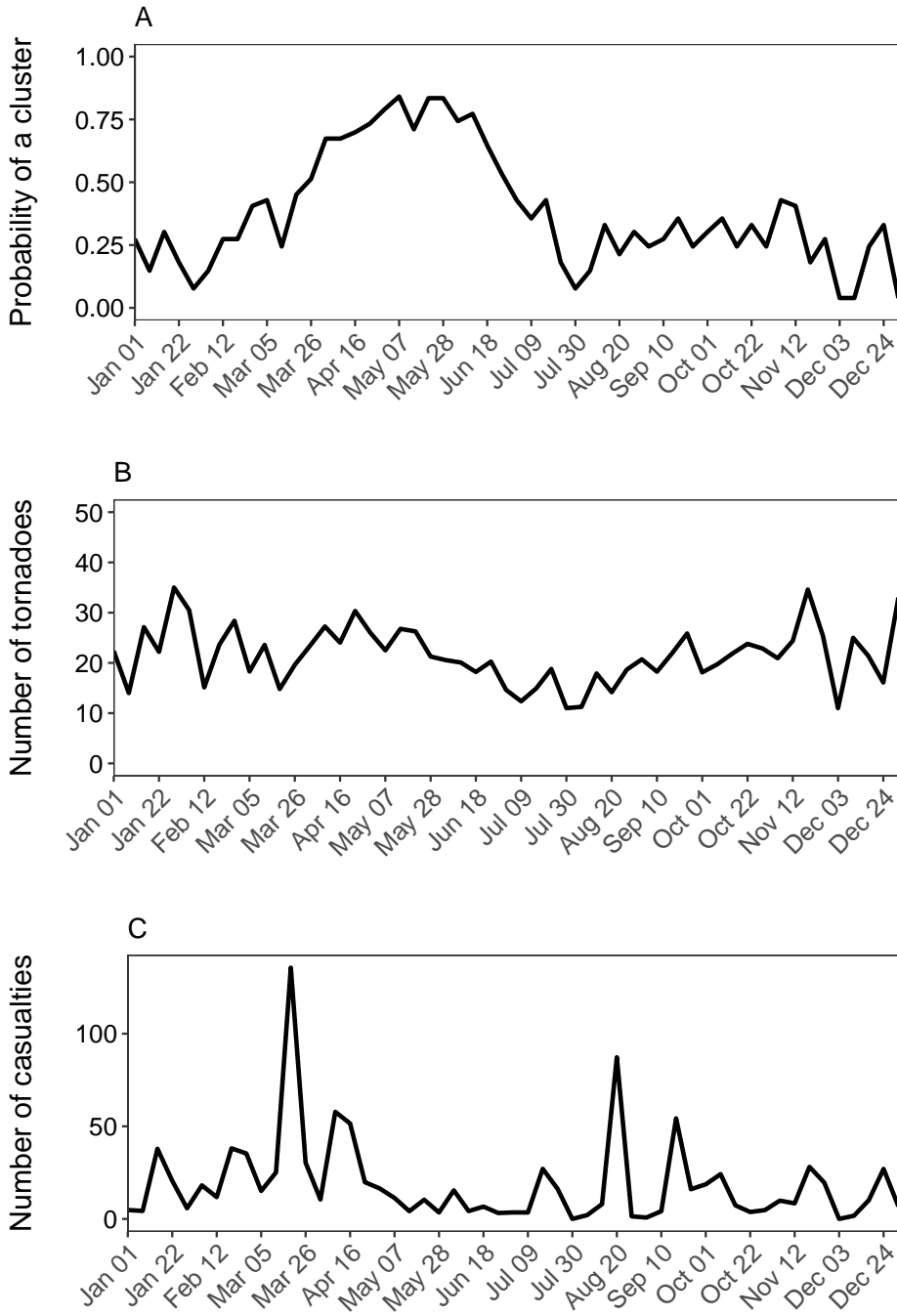
430 **Fig. 9.** Probability of at least 25 tornado casualties as a function of deep-layer bulk shear and CAPE
 431 and modulated by location for two *hypothetical* outbreaks, one centered over Sioux City,
 432 Iowa and the other centered over Birmingham, Alabama. The shallow-layer bulk shear is set
 433 to its mean value, year is set to 2018, and population is set to 4M. 35



434 FIG. 1. Example tornado clusters. Each point is the tornado genesis location shaded by EF rating. The black
 435 line is the spatial extent of the tornadoes occurring on that convective day and is defined by the minimum convex
 436 hull encompassing the set of genesis locations.



437 FIG. 2. Histograms of the number of clusters by number of tornadoes (A) and number of clusters by number of
 438 casualties (B). The histograms are right-truncated at 50 to show detail on the left side of the distributions. Only
 439 clusters with at least ten tornadoes are considered in this study.



440 FIG. 3. Probability of a cluster, average number of tornadoes per cluster, and average number of casualties per
 441 million people per cluster by week of the year.

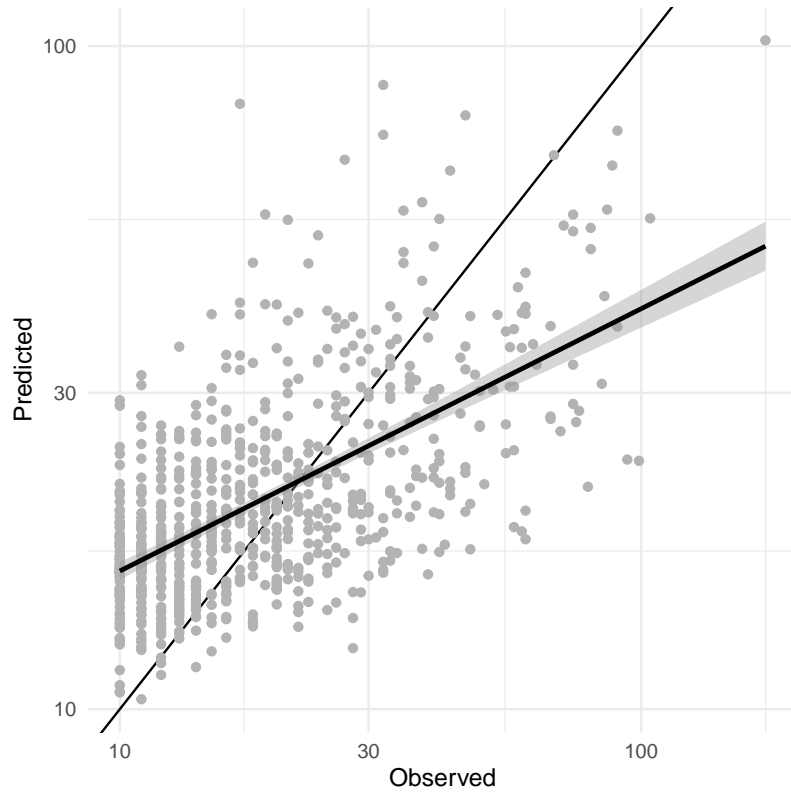
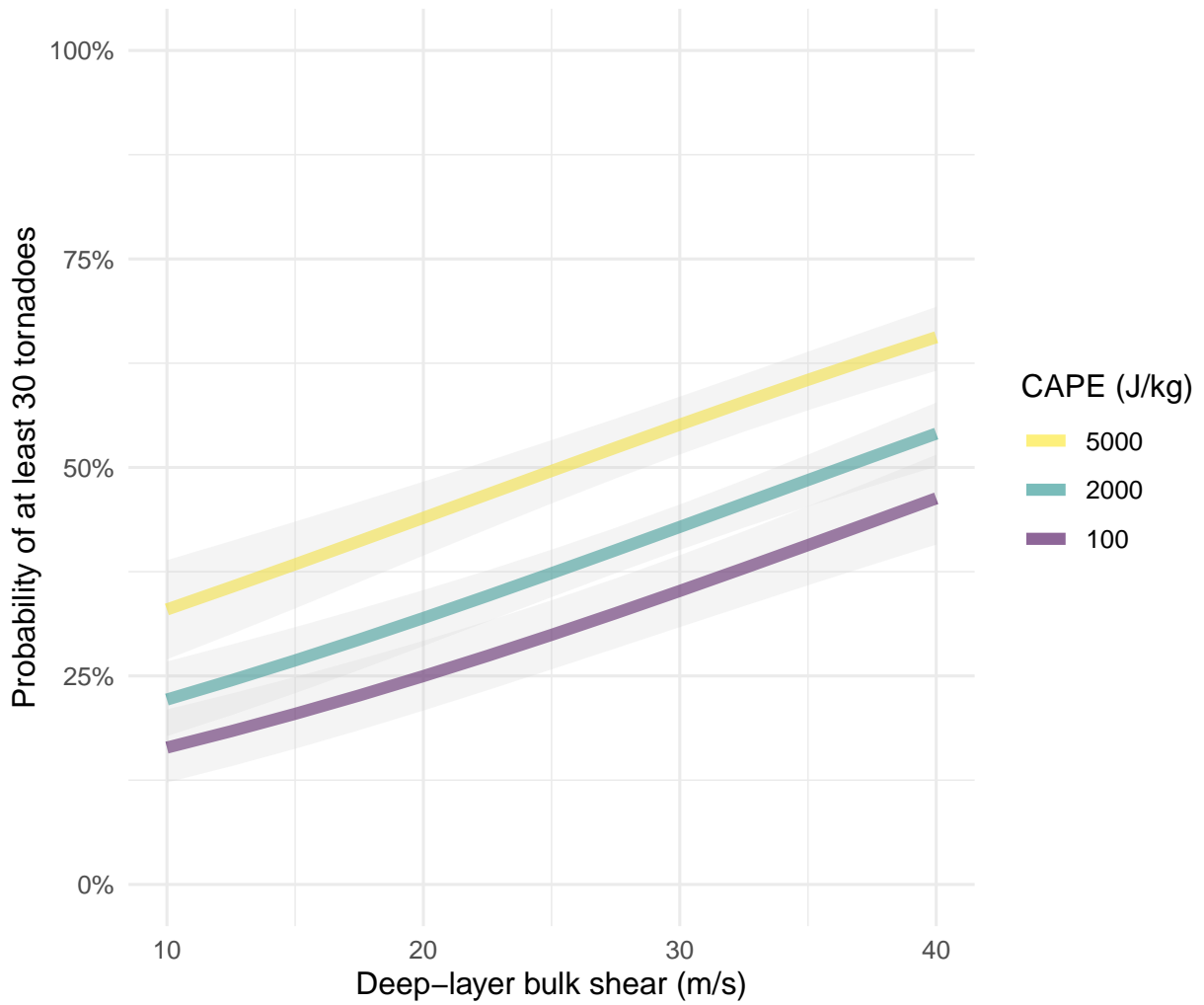
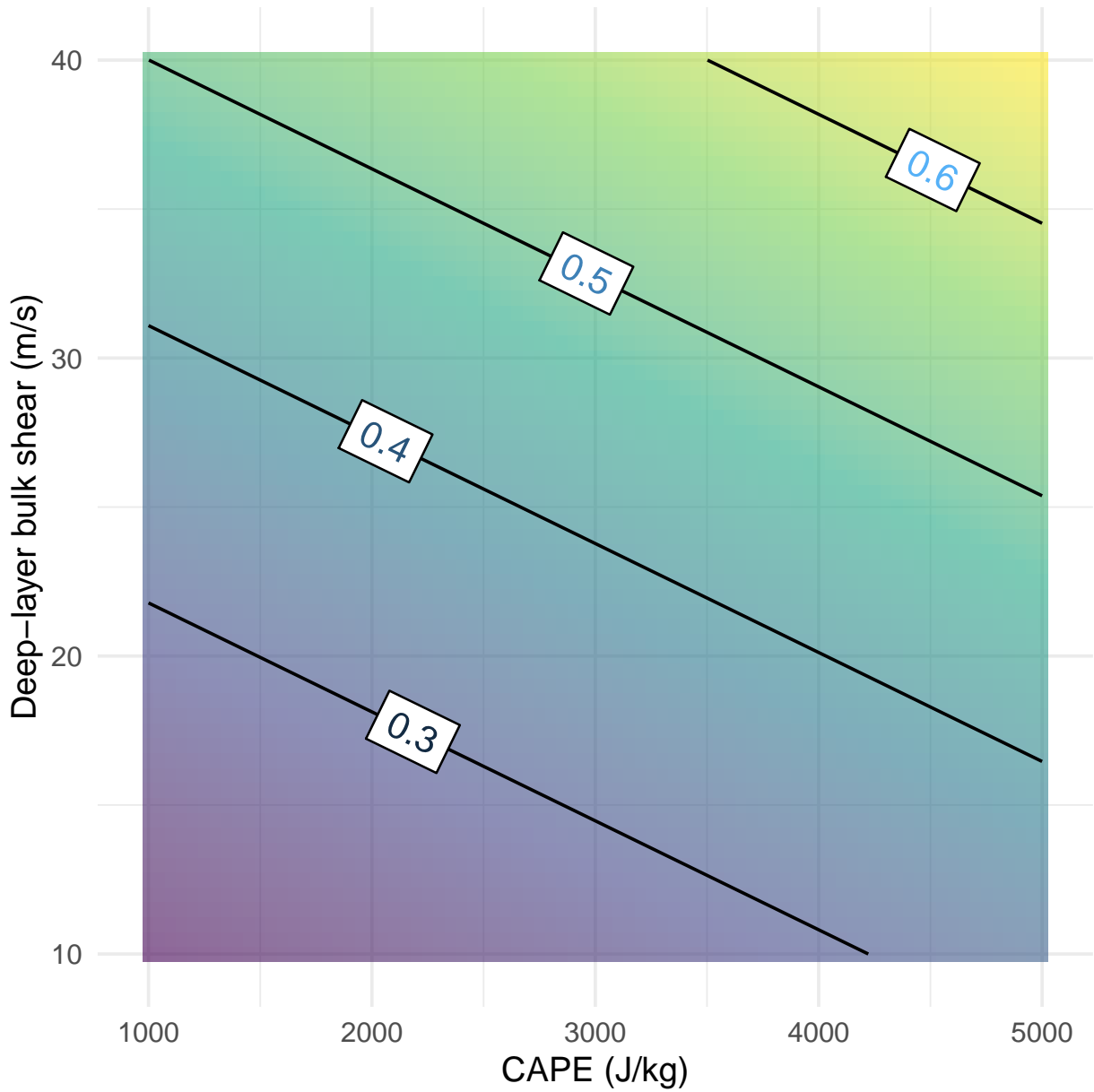


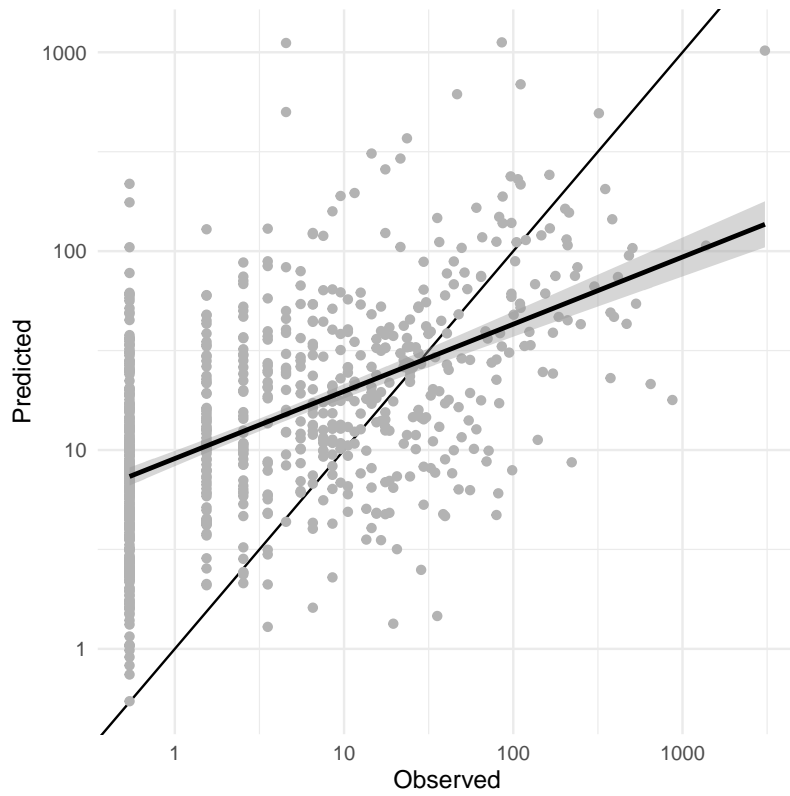
FIG. 4. Observed cluster-level tornado counts versus predicted rates from a negative binomial regression.



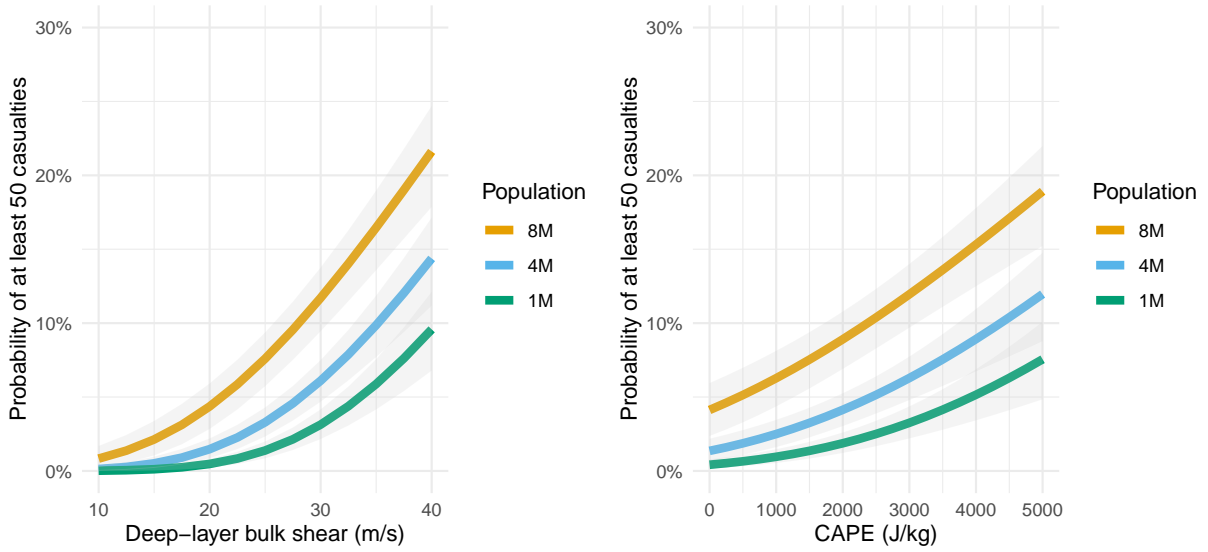
442 FIG. 5. Estimated probability of at least 30 tornadoes given an outbreak of at least ten tornadoes and the
 443 regression model. The predicted count from the model is a parameter in a negative binomial distribution with
 444 cluster area set at 400 000 km² and shallow-level bulk shear is set to its mean value.



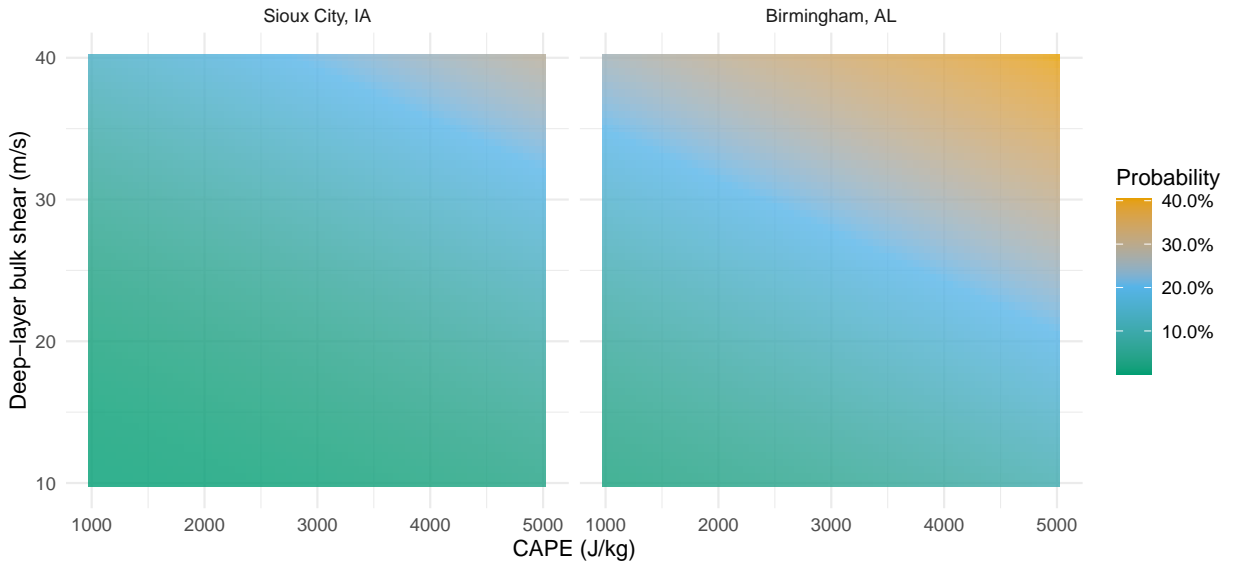
445 FIG. 6. Estimated probability of at least 30 tornadoes given an outbreak of at least ten tornadoes and the
 446 regression model across a range of CAPE and deep-layer bulk shear values holding the shallow-layer bulk shear
 447 at a mean value.



448 FIG. 7. Observed cluster-level casualty counts versus predicted rates from a negative binomial regression.
449 Clusters without casualties are plotted at the far left.



450 FIG. 8. Probability of at least 50 tornado casualties as a function of deep-layer bulk shear and CAPE and
 451 modulated by the number of people in harms way. The other variables are set at their mean values and year is set
 452 at 2018.



453 FIG. 9. Probability of at least 25 tornado casualties as a function of deep-layer bulk shear and
 454 modulated by location for two *hypothetical* outbreaks, one centered over Sioux City, Iowa and the other centered
 455 over Birmingham, Alabama. The shallow-layer bulk shear is set to its mean value, year is set to 2018, and
 456 population is set to 4M.